washing three times in ultra pure water for 10 min, the gels were stained in 1% silver nitrate solution for 5 min. The gels were washed in ultra pure water and in 1% sodium carbonate and formalin and sodium thiosulfate for 30 s each continuously. Development was performed in a solution consisting of 1% sodium carbonate and formalin and sodium thiosulfate until the clearest protein spots could be detected in each gel. Acetic acid (1%) was used to stop the development and the stained gels were then washed twice in ultra pure water for 5 min. These procedures were performed by using one container and silver stain kit (Atto, Tokyo, Japan) to compare with gels of normal and tumor samples under the same conditions.

2.5 Image analysis

The positions of the protein spots on the gels of OSCC tissues and surrounding normal tissues were recorded by using an Agfa ARCUS 1200^{TM} image scanner (Agfa-Gevaert NV, Mortsel, Belgium) and analyzed with Image Master software (Image Master 2D Platinum ver. 5.0, Amersham Biosciences AB, Uppsala, Sweden). The intensity of the cancer tissue spots was compared with those of corresponding normal tissues. Spots stained at different intensities were excised from the gels and stored in 100 μL of ultra pure water at –80°C as samples for MS analysis.

2.6 In-gel digestion

The silver stain was destained from the gel piece in a solution containing 30 mM potassium ferricyanide and 100 mM sodium thiosulfate for 10 min. After discarding the solution, 100 μL of ultra pure water was added to the tubes and vortexed gently and left for 5 min. This process was repeated three times. After discarding the water, 250 μL of solution containing 50% ACN, 50 mM ammonium bicarbonate, and 5 mM DTT were added and vortexed gently and left for 10 min. This process was repeated twice. The gel piece was dehydrated twice in 100% ACN for 30 min, and then re-swollen with an in-gel digestion reagent containing 10 μg/mL sequencing grade-modified trypsin (Promega, Madison, WI, USA) in 30% ACN, 50 mM ammonium bicarbonate, and 5 mM DTT and incubated overnight at 30°C. The samples were lyophilized overnight using LABCONCO-LYPH-LOCK-1L Model 77400 (Labconco, Kansas, MO, USA). Lyophilized samples were dissolved in 0.1% formic acid.

2.7 HPLC and MS

Samples dissolved in 0.1% formic acid were centrifuged at 21 500 × *g* for 5 min and the supernatant was stored at –80°C as samples for MS until use. An Agilent 1100 LC/MSD Trap XCT (Agilent Technologies, Palo Alto, CA, USA) was used for HPLC and MS. Protein identification was performed in the Agilent Spectrum MILL MS proteomics workbench against the Swiss-Prot protein database search engine (http://kr.expasy.org/sprot/) and the MASCOT MS/MS IonsSearch engine (http://www.matrixscience.com/search_form_select.html). The Spectrum Mill workbench can search MS/MS spectra using an MS/MS ion search.

2.8 Statistical analysis

Expression levels of the proteins were quantified by analyzing the intensity of each spot with Image Master 2D Platinum ver. 5.0 (Amersham Biosciences AB). The differences in expression between normal and tumor tissue samples were analyzed by a Student's *t*-test. $p < 0.05$ was considered significant.

2.9 Western blot analysis

After SDS-PAGE containing 15 μg of protein in each well, gels were transferred electrophoretically onto PVDF membranes (Immobilon-P; Millipore, Bedford, MA, USA) and blocked overnight at 4°C with TBS containing 5% skimmed milk. Primary antibodies were anti-14-3-3 σ-, which is an affinity-purified goat polyclonal antibody raised against a peptide mapping near the amino terminus of 14-3-3 σ of human origin (dilution range 1:200) (Santa Cruz Biotechnology, Santa Cruz, CA, USA), and an anti-actin rabbit polyclonal antibody as a loading control (dilution range 1:200) (Santa Cruz Biotechnology). For each, membranes were incubated overnight with the primary antibody at 4°C, washed three times with TBS containing 0.05% Tween-20 and once with TBS and then incubated with a HRP-conjugated secondary antibody (dilution range 1:2000) (ICN Pharmaceuticals, Aurora, OH, USA) for 1 h at room temperature, and developed with a chemiluminescence reagent (ECL^{TM} Western Blotting Detection Reagents; Amersham Biosciences, Buckinghamshire, UK).

2.10 Immunohistochemistry detection

Immunohistochemical analysis was performed by using the avidin–biotin amplification method and the Vectastain Elite ABC kit (Vector Laboratories, Burlingame, CA, USA) to estimate the protein expression levels of more cancerous tissues in four locations of the oral cavity. The used cancerous tissues were 5 buccal cancers, 7 oral floor cancers, 15 tongue cancers, and 11 gingival cancers resected for surgery or biopsy. Mouse monoclonal antibody anti-14-3-3 σ (Clone 1433S01) was purchased from Lab Vision (Fremont, CA, USA). Formalin-fixed and paraffin-embedded cancerous

tissue blocks were sliced to 4 μm each sections, which were incubated overnight with anti-14-3-3 σ antibody (3 μg/mL) at 4°C. Antigen retrieval was not performed. The antigen–antibody complex was visualized with a 3,3-diaminobenzine substrate kit for peroxidase (Vector Laboratories), and counterstained with hematoxylin. Nonneoplastic mouse skin epithelial tissue was used as a positive control. As negative controls, normal rabbit serum was used in place of primary antibodies. We performed the same staining without primary antibodies to confirm that the staining was not nonspecific caused by only secondary antibodies. They were classified into two groups: +, positive carcinoma cells and –, not immunoreactive. Hematoxylin and eosin staining was also performed by using the sections of the same area.

2.11 RT-PCR

Total RNA was isolated from gingival squamous cell carcinoma (SCC) tissues and adjacent nonmalignant gingival tissues by 300 μL Sepazol RNA I Super (Nacalai Tesque, Kyoto, Japan); raw tissue samples were homogenized with tissue Ruptor homoginizor (QIAGEN KK, Tokyo, Japan) for 40 s. Immediately, total RNA was isolated from primary tumor tissues by using RNeasy Fibrous tissue Mini Kit (QIAGEN KK). cDNAs were synthesized from 200 ng of total RNA using QuantiTectR Reverse Transcription. Reverse transcription was carried out for 15 min at 42°C, and then PCR was performed using the TOYOBO Blend Taq (TOYOBO, Osaka, Japan). For the determination of 14-3-3 σ cDNA content, a 25 μL reaction mixture consisted of 23 μL Blend Taq master mix, 0.5 μM each primer, and 1 μL of template cDNA were prepared. The PCR conditions were as follows: initial denaturation at 94°C for 2 min, and followed by cycles with denaturation at 94°C for 30 s, annealing at 55°C for 30 s, and extension at 72°C for 1 min, and then final extension at 72°C for 2 min. 14-3-3 σ specific primer was designed as follows: 5′-cggtgacgacaagaagcgcatca-3′ and 3′-ccccctcttccccggcgtt-5′ (310 bp). GAPDH specific primer was designed as 5′-gcatggccttccgtgtccc-3′ and 3′-gccagccccagcgtcaaag-5′. cDNA from Hela cell was used as a positive control, and water blank was used as a negative PCR control. PCR was performed using RT product without RT as template to check genomic DNA contamination.

3 Results

3.1 Detection of protein spots on 2-DE gels

Figure 1 is a typical 2-DE gel image of intracellular proteins from the oral floor SCC tissue and adjacent normal oral floor mucosa tissue. More than 300 protein spots were separated in a 8.5 × 6 cm^2 gel, with molecular weights

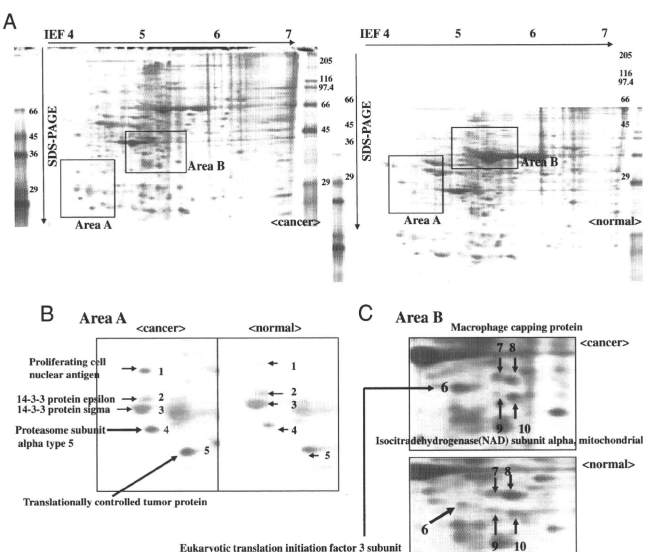

Figure 1. 2-DE gel pattern of representative oral cancer and normal oral mucosa. (A) 2-DE patterns of intracellular proteins in oral floor SCC tissue and normal oral floor mucosa tissue were visualized using silver stain. The 2-DE pattern of cancerous tissue is on the left and that of normal tissues is on the right. Each gel including 50 mg protein showed more than 300 spots. Ten protein spots were overexpressed more highly in OSCC samples than in normal samples. (B and C) Comparison of spots between cancer and normal tissue in the oral floor region. (B) Detailed 2-DE images of area A and (C) detailed 2-DE images of area B in (A). Detailed 2-DE image of cancerous tissue is in the left side and normal tissue is in the right side. Numbers with an arrow correspond to spot no. in Table 2.

ranging from 10 to 205 kDa and p*I* from 4 to 7. We performed proteomic analysis in four kinds of oral SCC tissues (buccal mucosa, oral floor, tongue, and gingiva). The patterns of the protein spots among these four types of SCCs were totally different, suggesting that different proteins and functional pathways may be involved in these four kinds of SCCs. We focused on the two areas in squares, whose areas have a comparatively similar pattern, and whose expression levels of protein spots are different between normal and tumor tissue samples (Fig. 1). Analysis of the expression level for each protein was performed by using Image Master 2D Platinum ver.5.0. Figure 2 shows the quantified intensity of each spot. Table 2 lists the proteins identified by LC-MS/MS and database searching. The protein of spots no. 2 and 3 was 14-3-3 protein family ε and σ, respectively. The protein of spots no. 7 and 8 was macrophage-capping protein. The protein of spots no. 9 and 10 was isocitrate dehydrogenase (NAD) subunit α. Figure 3 shows MS and MS/MS spectra of 14-3-3 σ (spot no. 3).

3.2 Immunoblot analysis of 14-3-3 σ in each location

Western blotting of 14-3-3 σ was performed for four locations, and its expression level of 14-3-3 σ was shown to be upregulated (Fig. 4).

3.3 Immunohistochemistry detection

As shown in Fig. 5, the majority of OSCC tissues were immunohistochemically positive for 14-3-3 σ proteins. The positive frequency of 14-3-3 σ protein is 100% (5/5) in buccal mucosa, 100% (7/7) in the oral floor, 100% (19/19) in the tongue, and 88% (16/18) in gingival mucosa. Panel A shows the images of normal buccal mucosa, mild dysplasia, carcinoma *in situ*, and buccal SCC. Panel B consists of images of normal gingival mucosa, poorly differentiated, moderately differentiated, and well-differentiated gingival SCC. As shown in panel C, diffuse immunoreactivity was

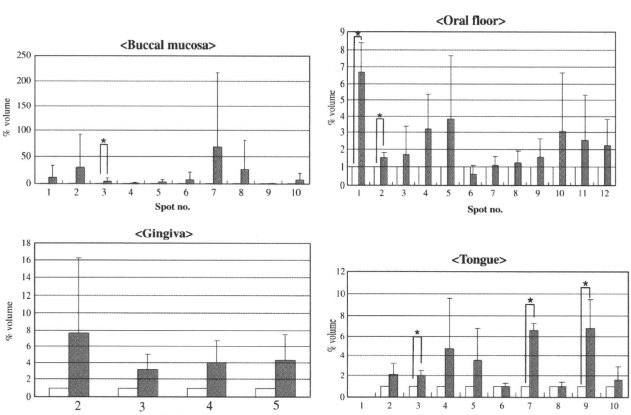

Figure 2. Expression analysis of ten proteins. Expression levels of proteins were quantified by analyzing % volume, *i.e.* the intensity and area of each spot. The white bars represent normal tissues and black bars represent cancer tissues. The differences in expression between cancer and normal tissue were analyzed by a Student's *t*-test. The data are expressed as the mean number of each protein ± SD. $^*p<0.05$ is significant.

Table 2. Identification of proteins that are expressed differentially between cancerous and noncancerous tissues

Spot	Mass (Da)/p*I*	Accession no.	Protein name
1	28 769/4.57	P12004	Proliferating cell nuclear antigen
2	29 174/4.63	P42655	14-3-3 protein epsilon
3	27 774/4.68	P31947	14-3-3 protein sigma
4	26 469/4.69	P28066	Proteasome subunit α type 5
5	19 595/4.84	P13693	Translationally controlled tumor protein
6	36 502/5.38	Q13347	Eukaryotic translation initiation factor 3 subunit
7	38 517/5.89	P40121	Macrophage-capping protein
8	38 517/5.89	P40121	Macrophage-capping protein
9	39 592/6.47	P50213	NAD subunit α, mitochondrial
10	39 592/6.47	P50213	NAD subunit α, mitochondrial

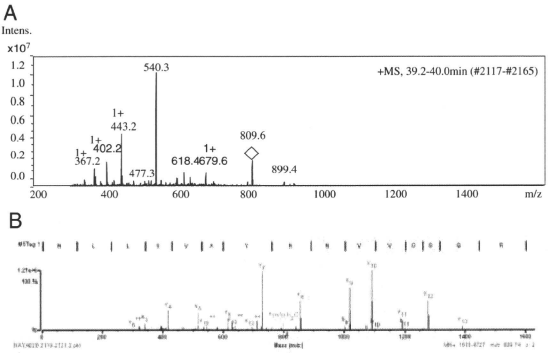

Figure 3. MS and MS/MS spectra of the tryptic digest of the 14-3-3 σ protein. (A) MS spectrum of tryptic digestion of the protein. The lozenge indicates the MS spectrum, precursor ion *m/z* (809.6), used for further MS/MS analysis. (B) MS/MS spectrum of precursor ion (*m/z* of spot noted in (A) processed with Spectrum MILL. Equivalent to (M+H)+ = 1618.472. Sequences of spots were determined in an Agilent Spectrum MILL MS proteomics workbench.

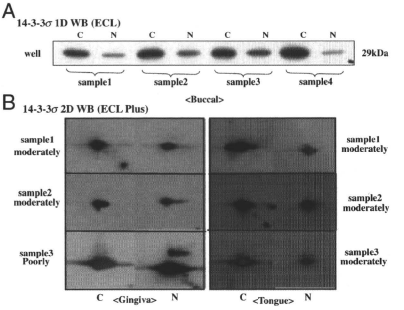

Figure 4. Immunoblot analysis of 14-3-3 σ protein. Lysate of 15 mg protein was loaded *per* well in four differential locations. In the buccal mucosa, 14-3-3 σ protein expression level was obviously upregulated at 29 kDa. There were differences in 14-3-3 σ protein expression levels between cancerous tissue and normal tissue in oral floor, gingival, and tongue samples.

also detected overall in the epithelium layer, and immunoreactivity of 14-3-3 σ was strongest in the poorly differentiated cancer region, its immunoreactivity becoming week with a transition from poorly, moderately, and well-differentiated cancer to normal tongue mucosa.

3.4 The expression level of 14-3-3 σ mRNA between gingival SCC tissues and adjacent nonmalignant gingival tissues

Next, semi-quantitative RT-PCR analysis for 14-3-3 σ mRNA was performed on gingival SCC tissues and adjacent nonmalignant gingival tissues. There was no significant increased expression of 14-3-3 σ mRNA in gingival SCC tissues (Fig. 6).

4 Discussion

The upregulated protein information can be produced by proteomic analysis for better understanding of carcinogenesis and pathogenesis in a global way, which in turn is a basis for the rational design of diagnostic and therapeutic methods.

The expression levels of HSP60, HSP27, α B-crystalline, ATP synthase β, calgranulin B, myosin, tropomyosin, and galectin 1 in oral tongue SCC, and those of SCC antigen, G protein, glutathione *S*-transferase, manganese and galectin 7 in oral buccal SCC were consistently found to be significantly altered in carcinoma tissues when compared with their paired normal mucosa [7, 8]. In this study, we analyzed the protein expression profile in 16 human samples of OSCC and corresponding noncancerous oral mucosa tissues. Eight proteins were identified as follows.

Proliferating cell nuclear antigen (PCNA) is an auxiliary protein of DNA polymerase δ and is involved in the control of eukaryotic DNA replication by increasing the polymerase's processibility during elongation of the leading strand. PCNA exists in the nucleus and forms a homotrimer. The overexpression of PCNA in cancer tissues was reported in some articles [28, 29].

14-3-3 σ and ε, which are 14-3-3 families, were the first signaling molecules to be identified as discrete phosphoserine/threonine-binding modules. This protein family, which includes seven isoforms (β, γ, ζ, σ, ε, η, ι) in human cells, plays critical roles in cell signaling events that control progress through the cell cycle, transcriptional alterations in response to environmental cues, and programmed cell death

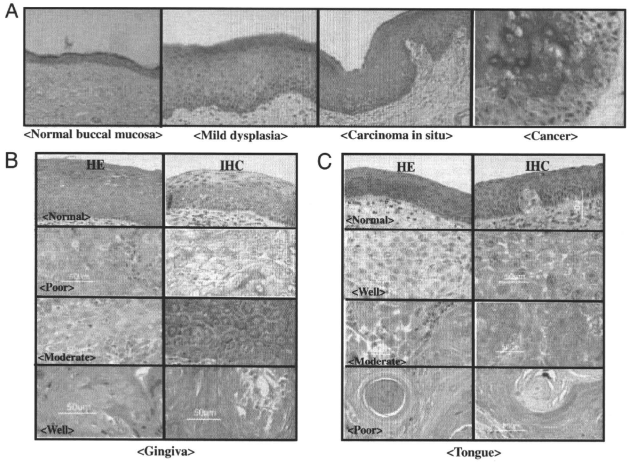

Figure 5. Immunohistochemistry of 14-3-3 σ in OSCC. Representative images of immunohistochemistry for 14-3-3 σ. (A, B, and C) show immunohistochemical images of buccal, gingival, and tongue SCC, respectively.

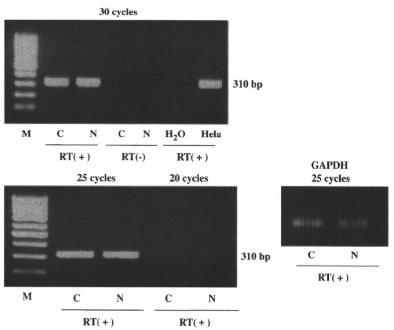

Figure 6. Semi-quantitative RT-PCR analysis for 14-3-3 σ in OSCC. Ethidium bromide-stained agarose gel shows the RT-PCR products corresponding to 14-3-3 σ (310 bp) transcripts. PCR was carried out for 20, 25, and 30 cycles. cDNA from Hela cell was used as a positive control, and water blank was used as a negative PCR control. PCR was performed using RT product without RT as template, to check genomic DNA contamination. C, cancerous tissue and N, nonmalignant tissue.

[30]. All 14-3-3 proteins bind to phosphoserine/phosphothreonine-containing peptide motifs corresponding to the sequences RSXpSXP or RXXXpSxP. 14-3-3 ε is a multifunctional regulator of the cell signaling processes mediated by tyrosine and tryptophan hydroxylases and protein kinase C. 14-3-3 σ was originally identified in squamous epithelium. 14-3-3 σ has been a major G2/M checkpoint control gene and maintains the dual-specificity phosphate Cdc25C [31]. Some articles demonstrated that its inactivation in various cancers occurs mostly by epigenetic hypermethylation and not by genetic change. Epigenetic silencing of 14-3-3 σ has been detected at a high frequency in the carcinoma of breast [32], ovary [33], endometrium [33], prostate [34], skin [35], lung [36] and liver [37], head and neck cancer cell lines [38]. Downregulation and epigenetic hypermethylation of 14-3-3 σ were reported for OSCC [39–41] and vulval squamous neoplasia [42]. In these cases tumor tissues were very close to HPV-infection. On the other hand, articles about the expression level of 14-3-3 σ showed some opposite results in each human cancer. Curiously, 14-3-3 σ is upregulated in lung carcinoma [43], head and neck squamous cell carcinoma [44], and oral buccal mucosa SCC [8]. From our results of 2-DE, IHC, and WB, 14-3-3 σ protein appears to be relatively more upregulated in cancer tissues than in normal tissues. Although we did not investigate HPV-infection state for patients, the opposite results may relate to HPV-infection state. In our case RT-PCR results did not show the downregulation of mRNA level for 14-3-3 σ. Chen *et al.*, also reported that strong overexpression was observed with both intact molecules as well as phosphorylated and truncated forms of 14-3-3 σ in the human buccal SCC [8]. In our study, 14-3-3 σ protein was not phosphorylated, but it did oxidize methionine at the 22nd, 26th, and 155th positions to become methionine-sulfoxide. Although the sequence for the fragment of (K)LAEQAERYEDMAAFMK(G) showed 1902.8724 Da (MH^+ Matched), 0.8630 Da (MH^+ Error) and

4.59e+009, that of (K)LAEQAERYEDmAAFmK(G) showed 1902.8724 Da (MH^+ Matched), 32.7530 Da (MH^+ Error) and 1.52e+008. Although the sequence for the fragment of (R)SAYQEAMDISKK(E) showed 1370.6620 Da (MH^+ Matched), 0.4707 Da (MH^+ Error) and 1.91e+009, that of (R)SAYQEAmDISKK(E) showed 1370.6620 Da (MH^+ Matched), 16.2507 Da (MH^+ Error) and 8.34e+008. As far as we know, only one article about carcinogenesis reported that in the serum of knockout mice deficient in hepatic AdoMet synthesis ($MAT1A^{-/-}$), as well as in patients with HCC, isoform 1 of three apolipoprotein A-I isoforms is upregulated in the serum. Characterization of isoform 1 by electrospray MS/MS revealed specific oxidation of methionine 85 and 216 to methionine sulfoxide while the sequence of the analogous peptides on isoforms 2 and 3 showed nonoxidized methionine residues [45]. The role of methionine residues in proteins has not been well defined, but a review of available studies leads to the conclusion that methionine, such as cysteine, functions as an antioxidant and as a key component of a system for regulating cellular metabolism. Methionine is readily oxidized to methionine sulfoxide by many reactive species. The oxidation of surface-exposed methionines thus serves to protect other functionally essential residues from oxidative damage [46]. This report agrees with our result. The 14-3-3 σ gene was overexpressed in head and neck SCC using a combination of complementary DNA subtraction and microarray analysis [44]. 14-3-3 σ is a multifunctional protein known to have 117 binding partners (*e.g.* proteins involved in oncogenic signaling, regulation of cytoskeletal dynamics, polarity, adhesion, mitogenic signaling, and motility) [47]. Upregulation of 14-3-3 σ protein is suggested to be caused by another function besides its function as a p53 target molecule.

Proteasome subunit α type 5 is one of the multicatalytic proteinase complexes, which is characterized by its ability to cleave peptides with Arg, Phe, Tyr, Leu, and Glu adjacent to the leaving group at neutral or slightly basic pH [48].

Translationally controlled tumor protein, known as an IgE-dependent histamine-releasing factor, is a growth-related tumor protein. Translationally controlled tumor protein is a housekeeping gene that is involved in tumor growth [49].

Eukaryotic translation initiation factor 3 subunit binds to the 40S ribosome and promotes the binding of methionyl-tRNAi and mRNA. The human tumor marker protein p150 was identified as the largest subunit of eukaryotic translation initiation factor 3 (also known as p170/p180). Its expression level is not only upregulated in many transformed cell lines, but also in several human cancers including breast, cervical, esophageal, and stomach carcinomas [50]. The function of p150 in cancer and initiation of translation are not well understood.

Macrophage capping protein is a unique member of the gelsolin–villin family of calcium-activated barbed end capping proteins which in micromolar Ca^{2+} also binds actin monomers and nucleates actin assembly. Unlike gelsolin, Macrophage capping protein cannot sever actin filaments, and its Ca^{2+}-dependent interaction with actin is completely reversible. This protein exists in macrophages and macrophage-like cells.

The NAD subunit α exists in mitochondria and shows catalytic activity: Isocitrate+NAD^+ = 2–oxoglutarate+CO_2+NADH. This protein has no report about the function according to carcinogenesis.

Upregulation of intracellular proteins in cancer tissues compared with surrounding normal tissues suggested two possibilities. One is the quantitative increase of protein produced. Another possibility is the acceleration of protein degradation. Therefore, it is also important to compare protein expression levels with gene expression levels.

In this study, we analyzed the protein expression profile in human 16 samples of OSCC. Further studies are required with more tissue samples to differentiate more clearly the protein expression level between normal and cancerous tissue. However, the proteins identified in this study may play an important role in human OSCC carcinogenesis and progression.

This work was supported in part by Grants-in-Aid from the Ministry of Education, Science, Sports, and Culture of Japan.

The authors have declared no conflict of interest.

5 References

[1] Gupta, P. C., Pindborg, J. J., Mehta, F. S., Comparison of carcinogenicity of betel quid with and without tobacco: an epidemiologic review. *Ecol. Dis.* 1982, *1*, 213–219.

[2] Moore, S. R., Johnson, N. W., Pierce, A. M., Wilson, D. F., Oral oncology: the epidemiology of mouth cancer: a review of global incidence. *Oral Dis.* 2000, *6*, 65–74.

[3] Froehlich, M., Epidemiologie der Lippen- und Mundschleim haut karzinome. *Med Aktuell.* 1991, *17*, 180–181.

[4] McDowell, J. D., An overview of epidemiology and common risk factors for oral squamous cell carcinoma. *Otolaryngol. Clin. North Am.* 2006, *39*, 277–294.

[5] Franceschi, S., Bidoli, E., Herrero, R., Munoz, N., Comparison of cancers of the oral cavity and pharynx worldwide: etiological clues. *Eur. J. Cancer (Oral. Oncol.).* 2000, *3*, 106–115.

[6] Lingen, M. W., Chang, K. W., McMurray, S. J., Solt, D. B. *et al.*, Overexpression of p53 in squamous cell carcinoma of the tongue in young patients with no known risk factors is not associated with mutations in exons 5–9. *Head Neck* 2000, *22*, 328–335.

[7] He, Q. Y., Chen, J., Kung, H. F., Yuen, A. P., Chiu, J. F., Identification of tumor-associated proteins in oral tongue squamouse cell carcinoma by proteomics. *Proteomics* 2004, *4*, 271–278.

[8] Chen, J., He, Q. Y., Yuen, A. P., Chiu, J. F., Proteomics of buccal squamouse cell carcinoma: the involvement of multiple pathways in tumorigenesis. *Proteomics* 2004, *4*, 2465–2475.

[9] Jain, M. R., Liu, T., Hu, J., Darfler, M. *et al.*, Quantitative proteomic analysis of formalin fixed paraffin embedded oral HPV lesions from HIV patients. *Open Proteomics J.* 2008, *1*, 40–45.

[10] Hiratsuka, H., Miyakawa, A., Nakamori, K., Kido, Y. *et al.*, Multivariate analysis of occult lymph node metastasis as a prognostic indication for patients with squamous cell carcinoma. *Cancer* 1997, *80*, 351–356.

[11] Kohama, G., Surgical management of carcinoma of the tongue and floor of the mouth with special reference to clinical stage and histological grade. *Oral Oncol.* 1995, *2*, 242–245.

[12] Hemmer, J., Thein, T., van Heerden, W. F.P., The value of DNA flow cytometry in predicting the development of lymph node metastasis and survival in patients with locally recurrent oral squamous cell carcinoma. *Cancer* 1997, *79*, 2309–2313.

[13] Asakage, T., Yokose, T., Mukai, K., Tsugane, S. *et al.*, Tumor thickness predicts cervical metastasis in patients with stage I/II carcinoma of the tongue. *Cancer* 1998, *82*, 1443–1448.

[14] Schena, M., Shalon, D., Davis, R. W., Brown, P. O., Quantitative monitoring of gene expression patterns with a complementary DNA microarray. *Science* 1995, *270*, 467–470.

[15] DeRisi, J., Penland, L., Brown, P. O., Bittner, M. L. *et al.*, Use of a cDNA microarray to analyse gene expression patterns in human cancer. *Nat. Genet.* 1996, *14*, 457–460.

[16] Golub, T. R., Slonim, D. K., Tamayo, P., Huard, C. *et al.*, Molecular classification of cancer: class discovery and class prediction by gene expression monitoring. *Science* 1999, *286*, 531–537.

[17] Brazma, A., Vilo, J., Gene expression data analysis. *FEBS Lett.* 2000, *480*, 17–24.

[18] Eisen, M. B., Spellman, P. T., Brown, P. O., Botstein, D., Cluster analysis and display of genome-wide expression patterns. *Proc. Natl. Acad. Sci. USA* 1998, *95*, 14863–14868.

[19] Mendez, E., Cheng, C., Farwell, D. G., Ricks, S. *et al.*, Transcriptional expression profiles of oral squamous cell carcinomas. *Cancer* 2002, *95*, 1482–1494.

[20] Ibrahim, S. O., Aarsaether, N., Holsve, M. K., Kross, K. W. *et al.*, Gene expression profile in oral squamous cell carcinomas and matching normal oral mucosal tissues from black Africans and white Caucasians: the case of the Sudan *vs* Norway. *Oral Oncol.* 2003, *39*, 37–48.

[21] O'Farrell, P. H., High-resolution two-dimensional electrophoresis of proteins. *J. Biol. Chem.* 1975, *250*, 4007–4021.

[22] Celis, J. E., Bravo, R., *Two-Dimensional Gel Electrophoresis of Protein: Methods and Applications*, Academic Press, London 1984.

[23] Dunn, M. J., Radola, B. J., in: Charambach, A., Dunn, M. J., Radola, D. J. (Eds.), Advances in Electrophoresis. Two-Dimensional Polyacrylamide Gel Electrophoresis, VHC, New York 1987, *1*, 1–110.

[24] Latner, A. L., Marshall, T., Gambie, M., Microheterogeneity of serum myeloma immunoglobulins revealed by a technique of high-resolution two-dimensional electrophoresis. *Electrophoresis* 1980, *1*, 82–89.

[25] Nakamura, K., Fujimoto, M., Tanaka, T., Fujikura, Y., Differential expression of nucleophosmin and stathmin in human T lymphoblastic cell lines, CCRF-CEM and JURKAT analyzed by two-dimensional gel electrophoresis. *Electrophoresis* 1995, *16*, 1530–1535.

[26] Fujimoto, M., Nagasaka, Y., Tanaka, T., Nakamura, K., Analysis of heat shock-induced monophosphorylation of stathmin in human T lymphoblastic cell line JURKAT by two-dimensional gel electrophoresis. *Electrophoresis* 1998, *19*, 2515–2520.

[27] Lowry, O. H., Rosebrough, N. J., Farr, A. L., Randall, R. J., Protein measurement with the folin phenol reagent. *J. Biol. Chem.* 1951, *193*, 265–275.

[28] Liu, Y., Chen, Q., Zhang, J. T., Tumor suppressor gene 14-3-3sigma is down-regulated whereas the proto-oncogene translation elongation factor 1delta is up-regulated in non-small cell lung cancers as identified by proteomic profiling. *J. Proteome Res.* 2004, *3*, 728–735.

[29] Li, C., Tan, Y. X., Zhou, H., Ding, S. J. *et al.*, Proteomic analysis of hepatitis B virus-associated hepatocellular carcinoma: identification of potential tumor markers. *Proteomics* 2005, *5*, 1125–1139.

[30] Yaffe, M. B., How do 14-3-3 sigma proteins work? – Gatekeeper phosphorylation and the molecular anvil hypothesis. *FEBS Lett.* 2002, *513*, 53–57.

[31] Peng, C. Y., Graves, P. R., Wu, Z ., Shaw, A. S., Piwnica-Worms, H ., Mitotic and G2 checkpoint control: regulation of 14-3-3 protein binding by phosphorylation of Cdc25C on serin-216. *Science* 1997, *277*, 1501–1505.

[32] Ferguson, A. T., Evron, E., Umbricht, C. B., Pandita, T. K. *et al.*, High frequency of hypermethylation at the 14-3-3 σ locus leads to gene silencing in breast cancer. *Proc. Natl. Acad. Sci. USA* 2000, *97*, 6049–6054.

[33] Mhawech, P., Benz, A., Cerato, C., Greloz, V. *et al.*, Down-regulation of 14-3-3 σ in ovary, prostate and endometrial carcinomas is associated with CpG island methylation. *Mod. Pathol.* 2005, *18*, 340–348.

[34] Lodygin, D., Diebold, J., Hermeking, H., Prostate cancer is characterized by epigenetic silencing of 14-3-3 σ expression. *Oncogene* 2004, *23*, 9034–9041.

[35] Lodygin, D., Yazdi, A. S., Sander, C. A., Herzinger, T., Hermeking, H., Analysis of 14-3-3 σ expression in hyperproliferative skin diseases reveals selective loss associated with CpG-methylation in basal cell carcinoma. *Oncogene* 2003, *22*, 5519–5524.

[36] Osada, H., Tatematsu, Y., Yatabe, Y., Nakagawa, T. *et al.*, Frequent and histological type-specific inactivation of 14-3-3 σ in human lung cancers. *Oncogene* 2002, *21*, 2418–2424.

[37] Iwata, N., Yamamoto, H., Sasaki, S., Itoh, F. *et al.*, Frequent hypermethylation of CpG islands and loss of expression of the 14-3-3 σ gene in human hepatocellular carcinoma. *Oncogene* 2000, *19*, 5298–5302.

[38] Vellucci, V. F., Germino, F. J., Reiss, M., Cloning of putative regulatory genes from primary human keratinocytes by substractive hybridization. *Gene* 1995, *166*, 213–220.

[39] Gasco, M., Bell, A. K., Heath, V., Sullivan, A. *et al.*, Epigenetic inactivation of 14-3-3 sigma in oral carcinoma: association with p16(INK4a) silencing and human papillomavirus negativity. *Cancer Res.* 2002, *62*, 2072–2076.

[40] Bhawal, U. K., Tsukinoki, K., Sasahira, T., Sato, F. *et al.*, Methylation and intratumoural heterogeneity of 14-3-3 sigma in oral cancer. *Oncol. Rep.* 2007, *18*, 817–824.

[41] Bhawal, U. K., Sugiyama, M., Nomura, Y., Kuniyasu, H., Tsukinoki, K., Loss of 14-3-3 sigma protein expression and presence of human papillomavirus type 16 E6 in oral squamous cell carcinoma. *Arch. Otolaryngol. Head Neck Surg.* 2008, *134*, 1055–1059.

[42] Gasco, M., Sullivan, A., Repellin, C., Brooks, L. *et al.*, Coincident inactivation of 14-3-3sigma and p16INK4a is an early event in vulval squamous neoplasia. *Oncogene* 2002, *21*, 1876–1881.

[43] Qi, W., Liu, X., Qiao, D., Martinez, J. D., Isoform-specific expression of 14-3-3 proteins in human lung cancer tissues. *Int. J. Cancer.* 2005, *113*, 359–363.

[44] Villaret, D. B., Wang, T., Dillon, D., Xu, J. *et al.*, Identification of genes overexpressed in head and neck squamous cell carcinoma using a combination of complementary DNA subtraction and microarray analysis. *Laryngoscope* 2000, *110*, 374–381.

[45] Fernández-Irigoyen, J., Santamaracute;a, E., Sesma, L., Muñoz, J. *et al.*, Oxidation of specific methionine and tryptophan residues of apolipoprotein A-I in hepatocarcinogenesis. *Proteomics* 2005, *5*, 4964–4972.

[46] Levine, R. L., Moskovitz, J., Stadtman, E. R., Oxidation of methionine in proteins: roles in antioxidant defense and cellular regulation. *IUBMB Life* 2000, *50*, 301–307.

[47] Benzinger, A ., Muster, N ., Koch, H. B., Yates, J. R., III, Hermeking, H ., Targeted proteomic analysis of 14-3-3 sigma, a p53 effector commonly silenced in cancer. *Mol. Cell. Proteomics.* 2005, *4*, 785–795.

[48] Coux, O., Tanaka, K., Goldberg, A. L., Structure and functions of the 20S and 26S proteasomes. *Ann. Rev. Biochem.* 1996, *65*, 801–847.

[49] Chung, S., Kim, M., Choi, W., Chung, J., Lee, K., Expression of translationally controlled tumor protein mRNA in human colon cancer. *Cancer Lett.* 2000, *156*, 185–190.

[50] Lin, L ., Holbro, T ., Alonsco, G ., Gerosa, D ., Burger, M. M., Molecular interaction between human tumor marker protein p150, the largest subunit of eIF3, and intermediate filament protein K7. *J. Cell. Biochem.* 2001, *80*, 483–490.

